Magnetization-Induced Second Harmonic Generation in a Polar Ferromagnet

Y. Ogawa,[1] Y. Kaneko,[1] J. P. He,[1] X. Z. Yu,[1] T. Arima,[1,2] and Y. Tokura[1,3,4]

[1]*Spin Superstructure Project, ERATO, Japan Science and Technology Corporation (JST), AIST Tsukuba Central 4, Tsukuba 305-8562, Japan*

[2]*Institute of Materials Science, University of Tsukuba, Tsukuba 305-8573, Japan*

[3]*Correlated Electron Research Center (CERC), National Institute of Advanced Industrial Science and Technology (AIST), AIST Tsukuba Central 4, Tsukuba 305-8562, Japan*

[4]*Department of Applied Physics, The University of Tokyo, Tokyo 113-8656, Japan*

(Received 23 July 2003; published 28 January 2004)

Second harmonic generation (SHG) induced by spontaneous magnetization has been investigated for a polar ferromagnetic crystal of $GaFeO_3$. The Kerr rotation of the second harmonic light becomes gigantic with decreasing temperature below the magnetic transition temperature ($\approx$205 K), e.g., as large as 73° at 100 K. The magnetic domains can be visualized by using that large nonlinear Kerr rotation. The spectrum of the magnetization-induced SHG as measured indicates the two-photon resonant electronic process on a Fe^{3+} ion in the crystal.

DOI: 10.1103/PhysRevLett.92.047401 PACS numbers: 78.20.Ls, 42.65.Ky, 75.60.Ch

Spontaneous electric polarization in a solid with broken space-inversion symmetry leads to the second-order nonlinear optical effects, e.g., second harmonic generation (SHG) [1]. On the other hand, spontaneous magnetization in a ferromagnet breaks the time-reversal symmetry, producing nonreciprocal magneto-optical effects, such as the magneto-optical Kerr effect and Faraday rotation [2]. When the time-reversal and space-inversion symmetries are both broken simultaneously in a material, new optical phenomena are expected to show up. One such example is the magnetization-induced second harmonic generation (MSHG), namely, the phenomenon that the magnetization (M) along the specific direction activates the originally silent tensor component(s) for the second-order nonlinear optical susceptibility, causing the M-dependent SHG [3].

Up to now, the MSHG phenomena have been observed for surfaces or interfaces of ferromagnetic materials (thin films) [3,4] or otherwise for polar antiferromagnets [5]. In the former case, the space inversion is broken only at surfaces or interfaces, yet the magnetization direction can be easily reversed and hence the nonlinear magneto-optical Kerr effect (NOMOKE), i.e., the field-direction dependent rotation of the polarization of the second harmonic (SH) light, is observed. On the other hand, in a polar antiferromagnet such as $YMnO_3$ and related crystals, the centrosymmetry is broken as a whole of the bulk crystal. In this case, some specific tensor elements of second-order nonlinear optical susceptibility are induced by the presence of the ordered spin moment in the antiferromagnetic state, which enables one to visualize the antiferromagnetic domain structure as well as the ferroelectric one of the crystal by an SHG imaging technique [6].

As the natural extension of these studies, the MSHG in a bulk *polar ferromagnet*, which has never been reported to the best of our knowledge, would be quite interesting, since we may expect gigantic NOMOKE. In this Letter, we have investigated the MSHG and NOMOKE of a single crystal of $GaFeO_3$, which is quite a rare example where the ferromagnetism and the pyroelectricity (electric polarization) can coexist in a bulk form. Taking both advantages of the magnetization reversibility (ferromagnetism) and the bulk electric polarization, we could demonstrate the gigantic Kerr rotation of the SH light and image the magnetic domains which are subject to the magnetic field. It is thus shown that the MSHG method is a powerful tool to observe the domain structure in the multiferroic material. We have also investigated the electric origin of the MSHG of $GaFeO_3$ in terms of the MSHG spectroscopy.

$GaFeO_3$ is a polar ferromagnet which was innovated by Remeika [7]. The crystal structure is depicted in Fig. 1(a). We could grow a large single crystal by a floating-zone method [10]. According to the structural analysis of the grown crystal [11], the octahedral sites (occupancy) are

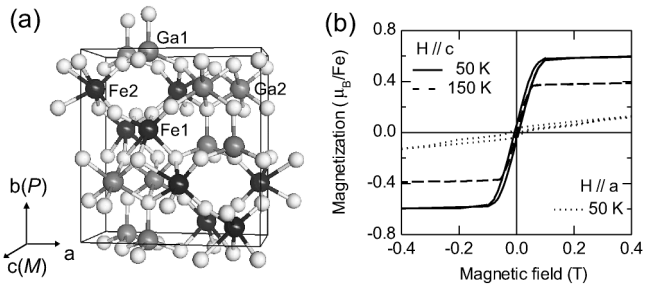

FIG. 1. (a) Crystal structure of $GaFeO_3$. Black, gray, and white balls indicate iron, gallium, and oxygen ions, respectively. Orthorhombic unit cell with the lattice constants a = 8.72, b = 9.37, and c = 5.07 Å, and the space group $Pc2_1n$ is shown by black lines [8,9]. (b) Temperature dependence of magnetization curves. The magnetic field is applied along the c (50 and 150 K) and a axes (50 K).

 0031-9007/04/92(4)/047401(4)$22.50

occupied by Fe (77% at the Fe1 site and 70% at the Fe2 site) and Ga (65% at the Ga2 site), while tetrahedral sites are mostly occupied by Ga (82% at the Ga1 site). The magnetic transition temperature T_C of the crystal is about 205 K. Figure 1(b) shows the magnetization curves. Magnetization along the c axis (easy axis) saturates at 0.1 T (50 K) and 0.05 T (150 K), respectively.

At first, we show the MSHG in a $GaFeO_3$ crystal. An exciting light source was a Ti:sapphire regenerative amplifier system (1.55 eV, 130 fs, 1 kHz). s-polarized [$\vec{E}(\omega) \parallel a$ axis] fundamental light was irradiated on the ac surface of the crystal with the angle of incidence being 26°, as shown in Fig. 2(a). The generated SH light was analyzed by a polarizer and detected with a photomultiplier tube and a boxcar averager. External magnetic fields of ±0.35 T applied along the c axis were large enough to revert the magnetization as shown in Fig. 1(b).

The space group of $GaFeO_3$ changes from $Pc2_1n$ in the paramagnetic phase to $Pc\underline{2_1}n$ in the ferromagnetic phase with the spontaneous magnetization along the c axis. Here we take the x, y, and z axes parallel to the a, b, and c axes of the crystal. Upon the irradiation of

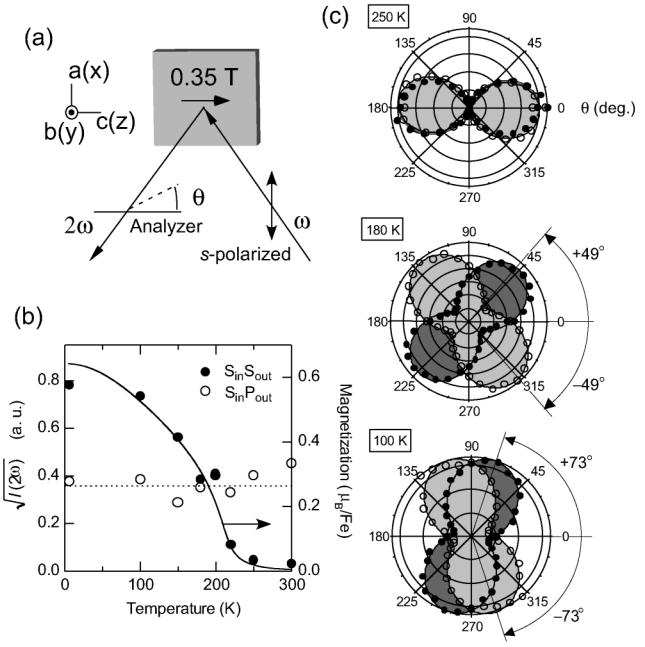

FIG. 2. (a) Experimental configuration for the measurement of the Kerr rotation of SH light in a $GaFeO_3$ crystal. (b) Square root of SH intensity $\sqrt{I(2\omega)}$ in $S_{in}S_{out}$ (solid circles) and $S_{in}P_{out}$ (open circles) configurations as a function of temperature. A solid line represents the magnetization in a magnetic field of 0.35 T applied parallel to the c axis (magnetic easy axis). A dotted line is merely the guide for the eyes. (c) Analyzer-angle dependence of SH intensity at 100 K, 180 K ($T < T_C$), and 250 K ($T > T_C$). Analyzer angles θ of 0° and 90° stand for p- and s-polarized SH light, respectively. Solid and open circles indicate the SH intensity for $+z$ and $-z$ directions of the magnetic field, respectively.

s-polarized [$\vec{E}(\omega) \parallel x$ axis] light, generated nonlinear polarization $\vec{P}(2\omega)$ is given by [12]

$$\vec{P}(2\omega) = \epsilon_0 \begin{pmatrix} \chi^m_{xxx} \\ \chi^{cry}_{yxx} + \chi^m_{yxx} \\ 0 \end{pmatrix} E^2_x(\omega). \quad (1)$$

χ^{cry}_{yxx} is a tensor element of $\chi^{(2)}$ of $GaFeO_3$, arising from the presence of the polarization along the b axis. The sign of χ^m_{xxx} depends on the direction of magnetization. On the other hand, the time-reversal operation does not change the sign of χ^m_{yxx}. These susceptibilities are complex in the presence of absorption. The square root of SH intensity $\sqrt{I(2\omega)}$ is proportional to $|\chi^m_{xxx}||E_x(\omega)|^2$ for the s-polarized component ($S_{in}S_{out}$ configuration) and $|\chi^{cry}_{yxx} + \chi^m_{yxx}||E_x(\omega)|^2$ for the p-polarized one ($S_{in}P_{out}$ configuration), respectively. Figure 2(b) shows the temperature dependence of $\sqrt{I(2\omega)}$ in $S_{in}S_{out}$(solid circles) and $S_{in}P_{out}$ (open circles) configurations. A solid line in the figure represents the magnetization in a magnetic field of 0.35 T applied parallel to the $c(z)$ axis. Note that the s-polarized component $|\chi^m_{xxx}|$ is proportional to the magnetization. On the other hand, the p-polarized component $|\chi^{cry}_{yxx} + \chi^m_{yxx}|$ least changes with temperature. This indicates that χ^m_{yxx} is negligibly small compared with the χ^{cry}_{yxx}.

Analyzer-angle (θ) dependence of SH light, which represents the nonlinear Kerr rotation, is shown at various temperatures, 250, 180, and 100 K, in Fig. 2(c). Analyzer angles of 0° and 90° stand for p- and s-polarized SH lights, respectively. Solid and open circles indicate the SH intensity for $+z$ and $-z$ directions of the applied magnetic field (0.35 T), respectively. At 250 K ($T > T_C$), the observed SH light is completely p polarized, as expected from vanishing magnetic components, χ^m_{xxx} and χ^m_{yxx}. However, the polarization of SH light rotates depending on the direction of the magnetic field when temperature is decreased below T_C. The nonlinear Kerr rotation angle ϕ becomes gigantic in this material with decreasing T below T_C, e.g., 49° at 180 K and 73° at 100 K, respectively [13].

Imaging of the magnetic domain structure can be done by using such a large nonlinear Kerr rotation. An exciting fundamental light (1.55 eV, 130 fs, 1 kHz) was focused on the ac surface of a crystal with a spot size of about 1 mm in diameter. The crystal was demagnetized by the ac method [14] after being cooled 150 K. The nonlinear Kerr rotation with the incidence angle of 26° at this temperature is as large as 60°. Reflected SH light was separated from fundamental light by bandpass filters, and its spatial variation was detected by a cooled charge-coupled-device camera. A typical exposure time was 30 min. However, the sensitivity would be an order of magnitude improved if we tuned the fundamental photon energy to the resonant condition, e.g., 1.8 eV, as described later.

Figure 3(a) shows a surface topographic image. The fundamental light was p polarized and the analyzer angle for the SH light was 0° ($P_{\text{in}}P_{\text{out}}$ configuration). The surface of the crystal is almost flat and no significant structure has been observed. Upon the irradiation of s-polarized fundamental light, the polarization of the SH light rotates as shown in Fig. 2(c). The image shown in Fig. 3(b) was taken with the analyzer angle θ being 45° [$S_{\text{in}}(S+P)_{\text{out}}$ configuration], and the bright region should correspond to the magnetic domain with the magnetization along the $-z$ direction. When the analyzer is rotated to 135° [$S_{\text{in}}(S-P)_{\text{out}}$ configuration], the bright and dark regions are exchanged as shown in Fig. 3(c), and the bright region indicates the $+z$ magnetic domains. Every magnetic domain boundary always runs parallel to the c axis, that is, the direction of easy magnetization axis, although the domain structure varies depending on the details of the ac demagnetization procedure. These characteristics result from the large magnetic anisotropy and the small saturation magnetization as described in Fig. 1(b) [2]. The image shown in Fig. 3(d) is a composition of images 3(b) and 3(c) which are colored blue and red to indicate the $-z$ and the $+z$ direction of the domain magnetization, respectively. Figures 3(e) and 3(f) were taken in external magnetic fields of ±0.05 T along the c axis, respectively, and then processed by the same procedure as in Fig. 3(d). It is immediately noticed that the magnetization of the whole crystal is uniformly aligned along the direction of the magnetic field.

To investigate an electric origin of the nonlinear magneto-optical phenomena in $GaFeO_3$, the spectrum of MSHG was measured in the range of the SH photon energy $2\hbar\omega$ from 2.6 to 4.5 eV. An optical parametric oscillator pumped by a third harmonic of a Nd-doped yttrium-aluminum-garnet (Nd:YAG) laser was used as a source of the fundamental light. The pulse width and the repetition rate were 5 ns and 10 Hz, respectively. An experimental setup was similar to Fig. 2(a), and the angle of incidence was 5°. The crystal was irradiated by s-polarized fundamental light, and the s-polarized SH light was detected ($S_{\text{in}}S_{\text{out}}$ configuration). Therefore, only the magnetization-induced second harmonic (MSH) signal was observed, which is proportional to $|\chi^{m}_{xxx}|^2$. The MSH intensities of the $GaFeO_3$ crystal was normalized by the SH signal of α quartz as the reference to correct the spectral response of the detection system. The maximum intensity of the observed MSH in the $GaFeO_3$ was as large as 6% of that of α quartz.

Figure 4 shows the spectra of the MSH at 10 K (solid line) and 220 K (dotted line) and the optical density [one-photon absorption (OPA)] of the 40-μm-thick crystal at 10 K (dash-dotted line). The SH spectrum is plotted as a function of two-photon energy. The upper part of Fig. 4

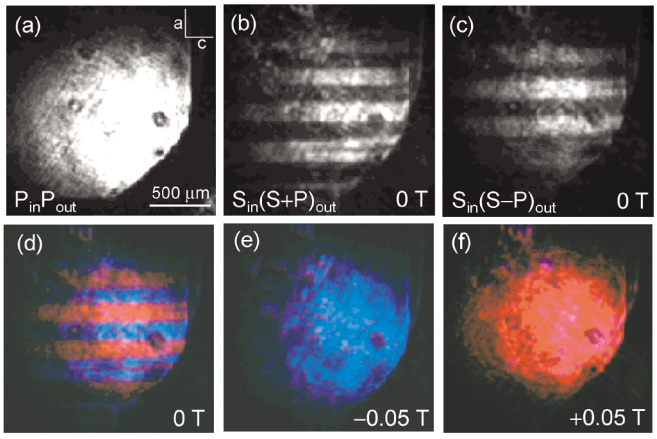

FIG. 3 (color). (a) Topographic image of the ac surface of the crystal as taken by the SH light in the nonmagnetic configuration, i.e., P_{in}-P_{out}. Magnetic domains aligned along the c axis were observed by reflected SH intensity in (b) $S_{\text{in}}(S+P)_{\text{out}}$ and (c) $S_{\text{in}}(S-P)_{\text{out}}$ configurations. With the former (latter) configuration, SHG intensity from domains which are magnetized along the $-z$ ($+z$) direction is much larger than from $+z$ ($-z$) magnetized domains. (d) Composition of images (b) and (c) which are colored blue and red to show magnetic domains with the magnetization direction of $-z$ and $+z$, respectively. In external magnetic fields of (e) -0.05 T and (f) $+0.05$ T along the c axis, the multidomain structure disappeared and the magnetization is aligned uniformly over the whole part of the crystal.

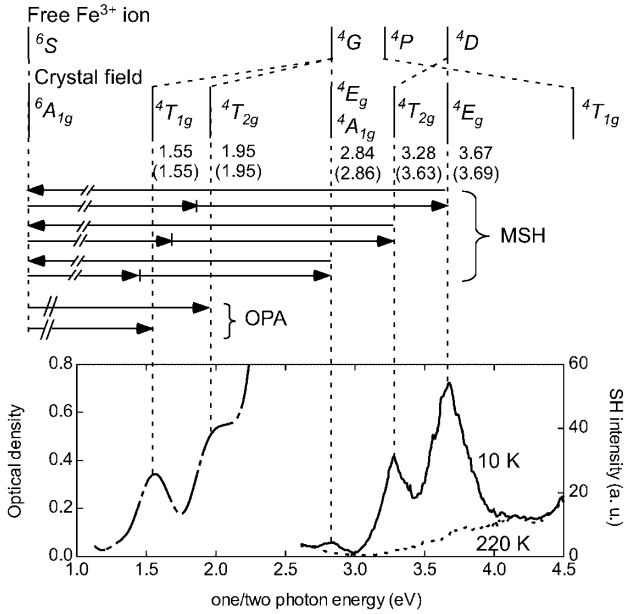

FIG. 4. Upper panel: energy levels of Fe^{3+} ions in free space and in an O_h octahedral crystal field. Middle panel: MSH and OPA processes. The observed (calculated) level energies are shown in units of eV. (See the text.) Lower panel: spectrum of MSHG (magnetization-induced $S_{\text{in}}S_{\text{out}}$ component) on the $GaFeO_3$ ac surface at 10 K (solid line) and 220 K (dotted line) and the OPA optical density of the 40-μm-thick crystal at 10 K (dash-dotted line). The SH spectrum is plotted for two-photon energy, i.e., photon energy of SH light.

depicts the energy levels of a Fe^{3+} ion in free space and in a regular octahedral (O_h) crystal field. The symmetry is lower in a real crystal, but the excited energy levels may be approximated as described in this diagram. Five d electrons of the Fe^{3+} ion constitute a high-spin ground state ($^6A_{1g}$) [15]. Two peaks are observed around 1.55 and 1.95 eV in the absorption spectrum and are assigned to the OPA bands from the ground state of Fe^{3+} to two lower lying excited states: $^6A_{1g} \rightarrow {}^4T_{1g}$ and $^6A_{1g} \rightarrow {}^4T_{2g}$ [16]. These absorption bands bear small oscillator strengths as they are barely allowed by spin-orbit coupling as well as by noncentrosymmetric crystal field [17]. The OPA spectrum above 2.3 eV could not be measured directly due to the intense charge transfer transition from the O $2p$ states to the Fe $3d$ states.

There are distinct three peaks in the MSH spectrum around 2.84, 3.28, and 3.67 eV at 10 K. These peaks disappear at 220 K ($>T_C$) in agreement with the result shown in Fig. 2(b). The fundamental photon energies (1.42, 1.64, and 1.84 eV) do not coincide with the peak energies of OPA bands (1.55 and 1.95 eV). One of the possible MSHG processes may be the magnon-assisted transition to the OPA bands. However, magnon Raman scattering could not be observed around 0.1–0.2 eV. Therefore, it is natural to consider that these peaks are in two-photon resonance with intra-atomic excited states of Fe^{3+}; two ^4E_g, $^4A_{1g}$, and $^4T_{1g}$ states as described in the middle panel of Fig. 4.

The energy values of these levels were calculated using the Tanabe-Sugano model [18], as shown as numerals (in units of eV) in parentheses in the middle panel of Fig. 4. The Racah parameters (B and C) and the crystal field energy ($10Dq$) were obtained so as to best reproduce all the energy values of the observed two OPA ($^4T_{1g}$ and $^4T_{2g}$) and three MSH (^4E_g, $^4A_{1g}$, and $^4T_{2g}$) peaks. The deduced parameters, $B = 0.119$ eV, $C = 0.335$ eV, and $10Dq = 1.69$ eV, are well in accord with those of other Fe^{3+} systems in an octahedral ligand field [18,19]. The good agreement between the observed and calculated level energies supports the present interpretation of the microscopic process of the MSHG in $GaFeO_3$.

In summary, we have demonstrated the magnetization-induced second harmonic generation in a polar ferromagnet $GaFeO_3$ crystal. The MSH intensity is as large as the bulk inherent SH intensity. Thus the nonlinear Kerr rotation angle becomes gigantic with decreasing temperature below the magnetic transition temperature ($\approx$205 K): 49° at 180 K and 73° at 100 K, respectively. By making use of the large nonlinear Kerr rotation, the magnetic domain structure can be clearly visualized. The spectrum of MSHG has indicated that the MSHG signal is two-photon resonant with intra-atomic excited states of Fe^{3+}.

We thank T. Ogasawara, H. Okamoto, E. Hanamura, S. Iwai, J. H. Jung, Y. Onose, and M. Kubota for helpful discussions.

[1] Y. R. Shen, *The Principles of Nonlinear Optics* (J. Wiley and Sons, New York, 1984).
[2] L. D. Landau, E. M. Lifshitz, and L. P. Pitaevski, *Electrodynamics of Continuous Media* (Pergamon, Oxford, 1984).
[3] For a review, see K. H. Bennemann, *Nonlinear Optics in Metals* (Clarendon Press, Oxford, 1998).
[4] For giant nonlinear Kerr rotation, see, for example, B. Koopmans, M. G. Koerkamp, Th. Rasing, and H. van den Berg, Phys. Rev. Lett. **74**, 3692 (1995); for domain imaging, see V. Kirilyuk, A. Kirilyuk, and Th. Rasing, Appl. Phys. Lett. **70**, 2306 (1997).
[5] M. Fiebig, D. Fröhlich, B. B. Krichevtsov, and R. V. Pisarev, Phys. Rev. Lett. **73**, 2127 (1994); D. Fröhlich, S. Leute, V. V. Pavlov, and R. V. Pisarev, Phys. Rev. Lett. **81**, 3239 (1998).
[6] M. Fiebig, Th. Lottermoser, D. Fröhlich, A. V. Goltsev, and R. V. Pisarev, Nature (London) **419**, 818 (2002).
[7] J. P. Remeika, J. Appl. Phys. **31**, 263S (1960).
[8] E. A. Wood, Acta Crystallogr. **13**, 682 (1960).
[9] S. C. Abrahams and J. M. Reddy, Phys. Rev. Lett. **13**, 688 (1964); S. C. Abrahams, J. M. Reddy, and J. B. Bernstein, J. Chem. Phys. **42**, 3957 (1965).
[10] T. Arima *et al.* (unpublished).
[11] M. Kubota *et al.* (unpublished).
[12] R. R. Birss, *Symmetry and Magnetism* (North-Holland, Amsterdam, 1964).
[13] The physical origin of such a large ϕ is that $|\chi^m_{xxx}|$ is as large as or even larger than $|\chi^{cry}_{yxx}|$. The magnetic component $|\chi^m_{xxx}|$ in a $GaFeO_3$ crystal originates from the product of the local polarization and the local magnetic moment vectors at the respective Fe site, which is the troidal moment discussed by Popov *et al.* in the case of the magnetoelectric effect [Yu. F. Popov *et al.*, J. Exp. Theor. Phys. **87**, 146 (1998)]. This product is accumulated uniformly (not canceled) when summed over the whole Fe site, even though the spins are mostly coupled antiferromagnetically [10]. On the other hand, the nonmagnetic component $|\chi^{cry}_{yxx}|$ is proportional to summation of the local polarization, which is partially canceled out because the direction of the distortion is opposite at Fe1 and Fe2 sites as described in Fig. 1(a).
[14] In the present experiment, a vibrating ($\sim$10 Hz) magnetic field was applied along the c axis on the crystal, while decreasing its magnitude from 0.05 T to zero, at 150 K.
[15] R. B. Frankel *et al.*, Phys. Rev. Lett. **15**, 958 (1965).
[16] R. V. Pisarev, Sov. Phys. Solid State **7**, 158 (1965).
[17] S. Koide and M. H. L. Pryce, Philos. Mag. **3**, 607 (1958).
[18] Y. Tanabe and S. Sugano, J. Phys. Soc. Jpn. **9**, 753 (1954).
[19] L. J. Heidt, G. F. Koster, and A. M. Johnson, J. Am. Chem. Soc. **80**, 6471 (1959).